Published OnlineFirst December 22, 2009; DOI: 10.1158/0008-5472.CAN-09-1449

Cancer Research

Proapoptotic Activity of Bortezomib in Gastrointestinal Stromal Tumor Cells

Sebastian Bauer[1], Joshua A. Parry[2], Thomas Mühlenberg[1], Matthew F. Brown[2,3], Danushka Seneviratne[2,3], Payel Chatterjee[2], Anna Chin[2], Brian P. Rubin[6], Shih-Fan Kuan[4], Jonathan A. Fletcher[7], Stefan Duensing[2,5], and Anette Duensing[2,3,4]

Abstract

Gastrointestinal stromal tumors (GIST) are caused by activating mutations in the *KIT* or *PDGFRA* receptor tyrosine kinase genes. Although >85% of GIST patients treated with the small-molecule inhibitor imatinib mesylate (Gleevec) achieve disease stabilization, complete remissions are rare and a substantial proportion of patients develop resistance to imatinib over time. Upregulation of soluble, non–chromatin-bound histone H2AX has an important role in imatinib-induced apoptosis of GIST cells. Additionally, H2AX levels in untreated GIST are maintained at low levels by a pathway that involves KIT, phosphoinositide 3-kinase, and the ubiquitin-proteasome system. In this study, we asked whether bortezomib-mediated inhibition of the ubiquitin-proteasome machinery could lead to upregulation of histone H2AX and GIST cell death. We show that bortezomib rapidly triggers apoptosis in GIST cells through a combination of mechanisms involving H2AX upregulation and loss of KIT protein expression. Downregulation of *KIT* transcription was an underlying mechanism for bortezomib-mediated inhibition of KIT expression. In contrast, the nuclear factor-κB signaling pathway did not seem to play a major role in bortezomib-induced GIST cell death. Significantly, we found that bortezomib would induce apoptosis in two imatinib-resistant GIST cell lines as well as a short-term culture established from a primary imatinib-resistant GIST. Collectively, our results provide a rationale to test the efficacy of bortezomib in GIST patients with imatinib-sensitive or -resistant tumors. *Cancer Res; 70(1); 150–9.* ©2010 AACR.

Introduction

Gastrointestinal stromal tumors (GIST) are the most common mesenchymal tumors of the gastrointestinal tract. They are caused by activating mutations in the *KIT* or *PDGFRA* receptor tyrosine kinase genes (1–3) and can be effectively treated with the small-molecule kinase inhibitor imatinib mesylate (Gleevec; ref. 4). However, although >85% of patients with metastatic GIST benefit from imatinib therapy, complete responses are rare, and the majority of patients develop resistance to imatinib during the course of treatment (4–6).

Authors' Affiliations: [1]Sarcoma Center, West German Cancer Center, University of Essen Medical School, Essen, Germany; [2]Cancer Virology Program, University of Pittsburgh Cancer Institute, Hillman Cancer Center; [3]Cellular and Molecular Pathology Graduate Program and Departments of [4]Pathology and [5]Microbiology and Molecular Genetics, University of Pittsburgh School of Medicine, Pittsburgh, Pennsylvania; [6]Department of Molecular Genetics, Lerner Research Institute and Taussig Cancer Center, Cleveland, Ohio; and [7]Department of Pathology, Brigham and Women's Hospital, Boston, Massachusetts

Note: Supplementary data for this article are available at Cancer Research Online (http://cancerres.aacrjournals.org/).

Corresponding Author: Anette Duensing, University of Pittsburgh Cancer Institute, Hillman Cancer Center, Research Pavilion, Suite 1.8, 5117 Centre Avenue, Pittsburgh, PA 15213. Phone: 412-623-5870; Fax: 412-623-7715; E-mail: aduensin@pitt.edu.

doi: 10.1158/0008-5472.CAN-09-1449

Various second- and third-line therapies for GIST are being developed, with most of them targeting the oncogenically activated kinases *KIT* and *PDGFRA*. However, sunitinib (Sutent), a multitargeted compound that inhibits vascular endothelial growth factor receptor, RET, colony-stimulating factor-1 receptor, and FLT3 in addition to KIT/PDGFRA, is thus far the only Food and Drug Administration (FDA)–approved compound for the treatment of imatinib-resistant GIST (7–9). The most prevalent mechanisms of resistance to imatinib involve additional (secondary) mutations of *KIT* or *PDGFRA* that affect the conformation of the kinase domain (10–12), and only a subset of these imatinib-resistant mutations are sensitive to sunitinib. The efficacy of sunitinib and other ATP-competitive direct inhibitors of KIT/PDGFRA is further hampered by genomic heterogeneity of resistance mutations within each individual patient. Moreover, virtually all patients receiving imatinib or sunitinib for metastatic inoperable GIST have persistent measurable disease, indicating that KIT-inhibitory treatments may induce quiescence rather than apoptosis in a subset of cells, as suggested recently (13). It is therefore imperative to identify novel strategies for treating GIST, particularly using drugs that induce GIST cell apoptosis.

We have previously shown that upregulation of soluble histone H2AX induces apoptosis in imatinib-treated GIST cells (14). We found that in untreated GIST cells, H2AX levels are regulated by a pathway that involves KIT, phosphoinositide 3-kinase, and the ubiquitin-proteasome machinery. Hence, we ask here whether it would be possible to upregulate

Published OnlineFirst December 22, 2009; DOI: 10.1158/0008-5472.CAN-09-1449

levels of histone H2AX to induce GIST cell apoptosis by inhibiting its proteasomal degradation.

Bortezomib (Velcade) is a dipeptide boronic acid inhibitor of the 20S proteasome, which is FDA approved for the treatment of multiple myeloma and mantle cell lymphoma (15–17). The therapeutic activity of bortezomib results, in part, from impeding the degradation of proapoptotic factors, thereby inducing programmed cell death in neoplastic cells (18). In multiple myeloma, a key consequence of bortezomib treatment seems to be inhibition of the transcription factor nuclear factor-κB (NF-κB; refs. 16, 19).

In the present study, we tested the activity of bortezomib in GIST cells and found profound proapoptotic effects at concentrations similar to those showing activity against multiple myeloma *in vitro*. Bortezomib treatment increased histone H2AX expression and, unexpectedly, also resulted in a significant downregulation of KIT mRNA levels and subsequent protein expression. Inactivation of the NF-κB signaling pathway, however, did not play a major role in GIST cell apoptosis. Hence, our findings suggest that bortezomib has a dual mode of action against GIST cells involving upregulation of proapoptotic histone H2AX and downregulation of oncogenic KIT. Most importantly, bortezomib was active against imatinib-resistant GIST cells and a short-term culture derived from an imatinib-resistant GIST *in vitro*. Future studies are warranted to test the clinical effectiveness of bortezomib in GIST patients.

Materials and Methods

Cell culture and inhibitor treatments. The human GIST cell line GIST882 was derived from an untreated metastatic GIST and maintained in RPMI 1640 supplemented with 15% fetal bovine serum (Gemini BioProducts), 1% L-glutamine, 50 units/mL penicillin (Cambrex), and 50 μg/mL streptomycin (Cambrex) as described earlier (20). GIST430 and GIST48 were established from GISTs that had progressed during imatinib therapy after initial clinical response. As described previously (21), GIST430 and GIST48 cell lines have heterozygous primary *KIT* exon 11 mutations accompanied by secondary imatinib-resistant mutations in exons 13 and 17, respectively.

The short-term culture GIST004 was established from a patient with a clinically imatinib-refractory GIST that underwent surgery for removal of a progressing lesion at the University of Pittsburgh Medical Center Presbyterian Hospital, Pittsburgh, PA (Institutional Review Board protocol no. 0509050). The fresh tumor specimen was disaggregated with scalpels and incubated overnight at 37°C in a solution containing DNase and collagenase B. Following the enzymatic disaggregation, cells were collected by centrifugation, resuspended in RPMI 1640, and plated in 35-mm dishes. After growing to near confluency, cells were treated as indicated for 72 h and processed for protein extraction. Sequencing of the tumor and short-term culture DNA (22) revealed a primary *KIT* exon 11 deletion (del550-558) as well as a secondary imatinib-resistant mutation in *KIT* exon 14 (T670I), also known as the "gatekeeper mutation" (23).

Cells were treated with bortezomib (dissolved in DMSO; LC Laboratories) at concentrations ranging from 1 nmol/L to 10 μmol/L for up to 72 h. Imatinib mesylate (kindly provided by Novartis Pharma) was used at a final concentration of 1 μmol/L in DMSO. α-Amanitin (Sigma) was reconstituted in distilled water (dH_2O) and used at concentrations ranging from 0.1 to 5 μg/mL for up to 72 h. The IκB inhibitor Bay 11-7082 (Sigma), the heat shock protein-90 (HSP90) inhibitor 17-*N*-allylamino-17-demethoxygeldanamycin (17-AAG; EMD), as well as the proteasome inhibitors MG-132, MG-262 (both Boston Biochem), epoxomicin (EMD), and ZL_3VS (Biomol) were used at a final concentration of 1 μmol/L in DMSO for up to 72 h or as indicated. Human recombinant tumor necrosis factor α (TNF-α; Sigma) was reconstituted in PBS and used at 0.1 μmol/L for 24 h.

Immunologic and cell staining methods. Protein lysates of GIST monolayer cultures (24) were prepared by scraping cells into radioimmunoprecipitation assay buffer [1% NP40, 50 mmol/L Tris-HCl (pH 8.0), 100 mmol/L sodium fluoride, 30 mmol/L sodium pyrophosphate, 2 mmol/L sodium molybdate, 5 mmol/L EDTA, and 2 mmol/L sodium orthovanadate] containing protease inhibitors (10 μg/mL aprotinin, 10 μg/mL leupeptin, and 1 μmol/L phenylmethylsulfonyl fluoride). Lysates were incubated for 1 h with shaking at 4°C and then cleared by centrifugation for 30 min at 14,000 rpm at 4°C. Protein concentrations were determined by the Bradford assay (Bio-Rad). Thirty micrograms of protein were loaded on a 4% to 12% Bis-Tris gel (Invitrogen) and blotted onto a nitrocellulose membrane.

For immunofluorescence analysis, cells grown on coverslips were briefly washed in PBS and fixed in 4% paraformaldehyde in PBS for 15 min at room temperature. Cells were then washed in PBS and permeabilized with 1% Triton-X 100 in PBS for 15 min (room temperature) followed by washing in PBS and blocking with 10% normal donkey serum (Jackson Immunoresearch) for 15 min (room temperature). Cells were then incubated with primary antibodies overnight at 4°C in a humidified chamber and incubated for another 3 h at 37°C the next morning. After a brief wash in PBS, cells were incubated with FITC-anti-mouse or FITC-anti-rabbit secondary antibodies (Jackson Immunoresearch) for at least 2 h at 37°C, washed with PBS, and counterstained with 4′,6-diamidino-2-phenylindole (DAPI; Vector Laboratories). Cells were analyzed using an Olympus AX70 epifluorescence microscope equipped with a SpotRT digital camera.

Primary antibodies used for immunoblotting and immunofluorescence were poly(ADP-ribose) polymerase (PARP; Invitrogen/Zymed Laboratories), ubiquitin (BD Biosciences), mouse monoclonal phospho-H2AX S139 (Upstate/Millipore), H2AX (Bethyl Laboratories), phospho-KIT Y703 (Invitrogen/Zymed), KIT (DakoCytomation), phospho-RNA polymerase II S2 (Covance), phospho-RNA polymerase II S5 (Covance), RNA polymerase II (Covance), cyclic AMP response element-binding protein (CREB)–binding protein (CBP; Santa Cruz), p300 (Santa Cruz), phospho-IκB-α S32, IκB-α, phospho-NF-κB p65 S536, NF-κB p65 (all Cell Signaling), and actin (Sigma).

Published OnlineFirst December 22, 2009; DOI: 10.1158/0008-5472.CAN-09-1449

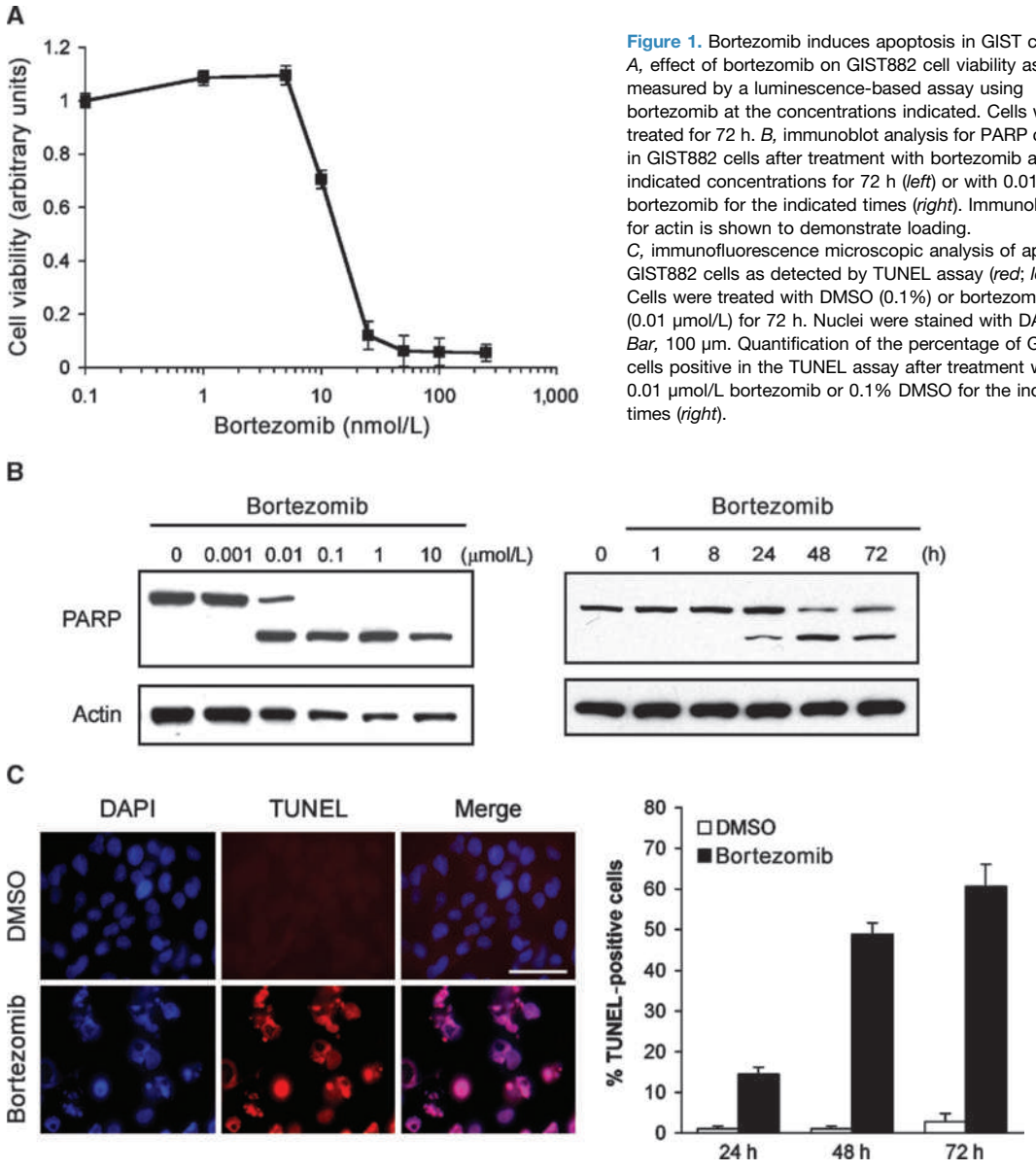

Figure 1. Bortezomib induces apoptosis in GIST cells. *A,* effect of bortezomib on GIST882 cell viability as measured by a luminescence-based assay using bortezomib at the concentrations indicated. Cells were treated for 72 h. *B,* immunoblot analysis for PARP cleavage in GIST882 cells after treatment with bortezomib at the indicated concentrations for 72 h (*left*) or with 0.01 μmol/L bortezomib for the indicated times (*right*). Immunoblot for actin is shown to demonstrate loading. *C,* immunofluorescence microscopic analysis of apoptotic GIST882 cells as detected by TUNEL assay (*red*; *left*). Cells were treated with DMSO (0.1%) or bortezomib (0.01 μmol/L) for 72 h. Nuclei were stained with DAPI. *Bar,* 100 μm. Quantification of the percentage of GIST882 cells positive in the TUNEL assay after treatment with 0.01 μmol/L bortezomib or 0.1% DMSO for the indicated times (*right*).

Apoptotic cells were visualized using the In situ Cell Death Detection kit (Roche Applied Sciences) according to the manufacturer's recommendations.

Reverse transcriptase-PCR and quantitative real-time reverse transcriptase-PCR. For reverse transcriptase-PCR (RT-PCR), cells were plated into p60 dishes, grown to 80% confluence, and treated with bortezomib (0.01 μmol/L), α-amanitin (1 μg/mL), and solvent controls for 48 h. RNA was extracted using the RNeasy Mini Kit (Qiagen) according to the manufacturer's protocol. RT-PCR was done using exon-overlapping, mRNA/cDNA-specific primers to KIT (forward, 5′-TCATGGTCGGATCACAAAGA-3′; reverse, 5′-AGGGGCTGCTTCCTAAAGAG-3′; Operon) and β-actin (forward, 5′-CCAAGGCCAACCGCGAGAAGAT-GAC-3′; reverse, 5′-AGGGTACATGGTGGTGCCGCCAGAC-3′) and the AccessQuick RT-PCR system from Promega. Cycling conditions were 50°C (45 min, reverse transcriptase reaction), 92°C (2 min, denaturation), 55°C (30 s, annealing), 62°C (45 s, extension), and 92°C (30 s, denaturation) for 20 cycles plus a final annealing step for 2 min at 62°C for KIT amplification or an annealing temperature of 44°C for β-actin on an Eppendorf Personal Cycler (Eppendorf).

For quantitative real-time RT-PCR (qRT-PCR), cDNA was transcribed by RT-PCR using random primers, and *KIT* cDNA was amplified and measured using TaqMan gene expression

Published OnlineFirst December 22, 2009; DOI: 10.1158/0008-5472.CAN-09-1449

assays (Applied Biosystems) and a real-time PCR system (LightCycler, Roche). *β-Actin* cDNA (also measured using TaqMan gene expression assay) served as reference gene for relative quantification.

In vitro *proliferation and apoptosis assays, flow cytometry.* Cell viability studies were done using the CellTiter-Glo luminescence-based assay (Promega) as described previously (21). For these studies, the cell lines were plated at 15,000 to 40,000 cells per well in a 96-well flat-bottomed plate (Falcon), cultured in serum-containing medium for 1 to 3 d, and then incubated for 72 h with bortezomib, imatinib, or DMSO-only solvent control. Luminescence was measured with a Veritas Microplate Luminometer (Turner Biosystems), and the data were normalized to the DMSO-only control group. All experimental points were measured in triplicate wells for each plate and were replicated in at least two plates.

Apoptosis was assessed by measuring caspase-3 and caspase-7 activity using the Caspase-Glo 3/7 luminescence-based assay (Promega) as described previously (21). Experimental conditions were as described above for the CellTiter-Glo studies.

For flow cytometry, cells were treated with bortezomib at the indicated concentrations for 24 or 48 h and resuspended in 100 μL of staining solution containing Annexin V-FITC (525 nm) and 7-AAD (675 nm) in HEPES buffer. After incubation at room temperature for 15 min, Annexin V–positive cells were estimated by flow cytometry, as described previously (21). Ten thousand events of each sample were acquired on a Beckman Coulter FC500 Flow Cytometer. Doublet discrimination was done with FL2 versus FL2 peak histogram.

Results

Bortezomib induces apoptosis in GIST cells. To determine whether bortezomib affects GIST cell proliferation and viability, GIST882 cells were treated with bortezomib at increasing concentrations. Substantial inhibition of proliferation was found at concentrations of 0.01 μmol/L and higher (Fig. 1*A*). To assess induction of apoptosis, GIST882 cells were treated with 0.001 to 10 μmol/L bortezomib for 72 hours and immunoblotted for PARP. A PARP cleavage fragment indicating apoptosis was detected in cells treated with concentrations as low as 0.01 μmol/L (Fig. 1*B, left*), which is the same concentration that led to a substantial reduction in cell growth and induction of apoptosis in multiple myeloma cells (16). A 72-hour time course experiment using this concentration (0.01 μmol/L) showed that induction of apoptosis is time dependent and started at 24 hours after beginning bortezomib treatment (Fig. 1*B, right*). Induction of apoptosis was also time-dependent when evaluated using the terminal deoxynucleotidyl transferase-mediated dUTP nick end labeling (TUNEL) assay (Fig. 1*C*). Quantification of apoptotic cells revealed a statistically significant increase of apoptotic cells to 14.5%, 48.9%, and 60.6% after 24, 48, and 72 hours of treatment, respectively, compared with control-treated cells that had corresponding apoptotic indices of 1%, 1%, and 2.8%, respectively ($P \leq 0.002$, $P \leq 0.0001$, and $P \leq 0.0006$, respectively; Fig. 1*C*). Taken together, these results show that bortezomib has profound proapoptotic activities in GIST cells.

Bortezomib upregulates histone H2AX and causes a rapid loss of KIT expression. To determine the mechanism of bortezomib-induced GIST cell apoptosis, we analyzed H2AX levels by immunoblotting and found that both phosphorylated and total histone H2AX protein expression increased in a dose- and time-dependent manner (Fig. 2). The increase in phospho-H2AX and total H2AX levels paralleled the increase in general ubiquitylation of proteins (data not shown). We also detected a second, higher molecular weight band (~24 kDa in size) that most likely corresponds to ubiquitylated histone H2AX, indicating that increased levels of H2AX after bortezomib treatment are possible mechanisms of apoptosis induction. When downregulating H2AX by small interfering RNA (siRNA), however, the percentage of surviving cells after bortezomib did not increase to the same extent seen after imatinib treatment (data not shown; ref. 14). These results suggest that additional mechanisms may be involved in bortezomib-induced GIST cell apoptosis.

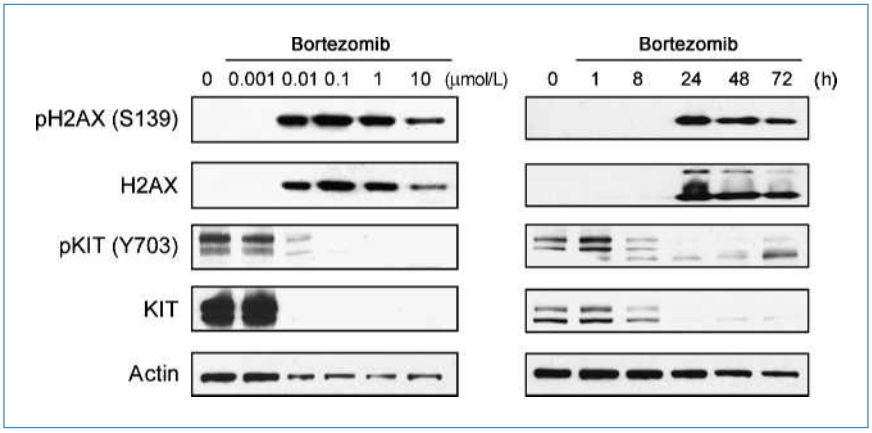

Figure 2. Bortezomib leads to upregulation of H2AX, but downregulates KIT. Immunoblot analysis of GIST882 cells treated with bortezomib at the indicated concentrations for 72 h (*left*) or with 0.01 μmol/L bortezomib for the indicated times (*right*) and probed for phospho-H2AX (S139) and total H2AX as well as phospho-KIT and total KIT. Immunoblot for actin is shown to demonstrate loading.

Published OnlineFirst December 22, 2009; DOI: 10.1158/0008-5472.CAN-09-1449

In line with this notion, we found that KIT protein expression levels were dramatically downregulated in a dose- and time-dependent manner after bortezomib treatment (Fig. 2). As expected, KIT phosphorylation decreased in parallel.

It is known that most GIST cells are dependent on continued KIT expression for their survival as evidenced by the fact that KIT knockdown by siRNA or downregulation of KIT using the HSP90 inhibitor 17-AAG readily causes GIST cell death (14, 21). Hence, downregulation of KIT could play a substantial role in bortezomib-induced apoptosis in GIST.

Bortezomib induces transcriptional downregulation of KIT. To further dissect the role of proteasome inhibition in bortezomib-induced GIST cell apoptosis, we treated GIST cells with several other proteasome inhibitors. Treatment with all compounds tested (MG-132, MG-262, epoxomicin, and ZL_3VS), which, like bortezomib, predominantly inhibit the chymotrypsin-like activity of the proteasome, led to an increase of phospho-H2AX and total H2AX levels as well as downregulation of KIT expression levels (Supplementary Fig. S1). These results suggest that the effect of bortezomib on GIST cells is most likely mediated by its ability to inhibit the chymotrypsin-like activity of the proteasome.

To analyze the events that are involved in the downregulation of KIT expression, we then tested whether bortezomib leads to transcriptional inhibition of *KIT*. *KIT* mRNA levels were substantially downregulated in GIST882 cells that were treated with 0.01 μmol/L bortezomib for 48 hours as shown by RT-PCR (Fig. 3*A, left*) and qRT-PCR (Fig. 3*A, right*). Remarkably, downregulation of *KIT* transcripts by 0.01 μmol/L bortezomib as determined by qRT-PCR was comparable to that observed when cells were treated with 1 μg/mL α-amanitin, a potent and selective inhibitor of RNA polymerase II.

We then tested the effects of bortezomib on the transcriptional machinery in GIST cells. Immunoblotting for RNA polymerase II phosphorylation at serine 2 (S2) of the tandem heptad repeats of its COOH-terminal domain showed a substantial decrease in phosphorylation after bortezomib treatment that was dose and time dependent (Fig. 3*B, left* and *middle*). Phosphorylation of RNA polymerase II (S2) is associated with transcriptional elongation (24). The same pattern was seen when probing for RNA polymerase II phosphorylation at serine 5 of the COOH-terminal domain, which occurs predominantly during transcriptional initiation. Inhibition of RNA polymerase II (S2) after bortezomib could also be visualized by immunofluorescence microscopy (Fig. 3*B, right*), showing loss of RNA polymerase II (S2) phosphorylation.

To directly test the effect of transcriptional inhibition on KIT expression in GIST cells, we performed a dose-response experiment treating GIST cells with increasing amounts of α-amanitin. As expected, α-amanitin led to a dose-dependent decrease of phosphorylation of RNA polymerase II (S2) and RNA polymerase II (S5; data not shown). Interestingly, α-amanitin treatment resulted in complete loss of KIT protein expression at concentrations of 1 μg/mL and higher, indicating that KIT is highly regulated at the transcriptional level (Fig. 3*C*).

In addition to downregulating RNA polymerase II, bortezomib also led to downregulation of the transcriptional coactivator CBP as shown by immunofluorescence staining (Fig. 3*D, left*). DMSO-treated cells (97.8%) showed positivity for CBP in the form of so-called nuclear speckles, whereas only 44.1% of the cells were positive when treated with 0.01 μmol/L bortezomib (Fig. 3*D, right*). Negative cells showed either a complete loss of CBP expression or redistribution of CBP into displacement foci that are associated with global transcriptional downregulation. The effect of bortezomib was comparable with treatment of GIST882 cells with 1 μg/mL α-amanitin (100% CBP positive in controls to 39.4% in cells treated with α-amanitin; Fig. 3*D, right*). Taken together, the global displacement of RNA polymerase II and CBP from chromatin throughout the nucleus suggests that bortezomib leads to a general transcriptional shutdown rather than to a specific loss of RNA polymerase II from the KIT promoter. Our results therefore indicate that bortezomib causes downregulation of KIT by inhibition of the transcriptional machinery.

Control experiments in which we treated GIST882 cells with imatinib or the HSP90 inhibitor 17-AAG revealed a rapid loss of KIT phosphorylation, but no change in KIT protein levels after imatinib (Supplementary Fig. S2*A, left*). In contrast, 17-AAG led not only to a loss of KIT phosphorylation but also to a loss of KIT protein expression (Supplementary Fig. S2*A, right*; ref. 21). Treatment with imatinib was associated with an inhibition of ongoing transcription (Supplementary Fig. S2*A–C*), whereas 17-AAG treatment resulted in an increase of RNA polymerase II phosphorylation at S5 (Supplementary Fig. S2*B, right*), indicating that bortezomib and imatinib differ substantially from 17-AAG with respect to the effects on the transcriptional machinery. In addition, imatinib led to an increase in the abundance of *KIT* mRNA, whereas 17-AAG resulted in a >2-fold decrease of *KIT* transcripts as determined by qRT-PCR (Supplementary Fig. S2*D*). The most likely explanation for these seemingly discrepant results is the effects of these compounds on posttranscriptional modifications that result in differences in mRNA stability.

To explore the role of NF-κB in bortezomib-induced GIST cell death, we treated GIST882 cells with the IκB inhibitor Bay 11-7082, which had no effect on apoptosis as judged by the lack of a PARP cleavage fragment (Supplementary Fig. S3*A*) or on levels of H2AX or KIT protein expression (Supplementary Fig. S3*A*). Furthermore, treatment of GIST882 cells with bortezomib had no effect on NF-κB signaling as measured by IκB-α and NF-κB phosphorylation in whole-cell lysates (Supplementary Fig. S3*B*). Most importantly, NF-κB p65 was cytoplasmic at baseline levels, indicating that it is not constitutively active in GIST882 cells (Supplementary Fig. S3*C* and *D*). Treatment with either bortezomib or Bay 11-7082 did not lead to a change in subcellular localization of NF-κB over a period of 72 hours (Supplementary Fig. S3*C* and *D*). By contrast, stimulation with TNF-α readily resulted in nuclear translocation of NF-κB (Supplementary Fig. S3*C* and *D*), thus indicating that the pathway is nevertheless functional in GIST882 cells.

Published OnlineFirst December 22, 2009; DOI: 10.1158/0008-5472.CAN-09-1449

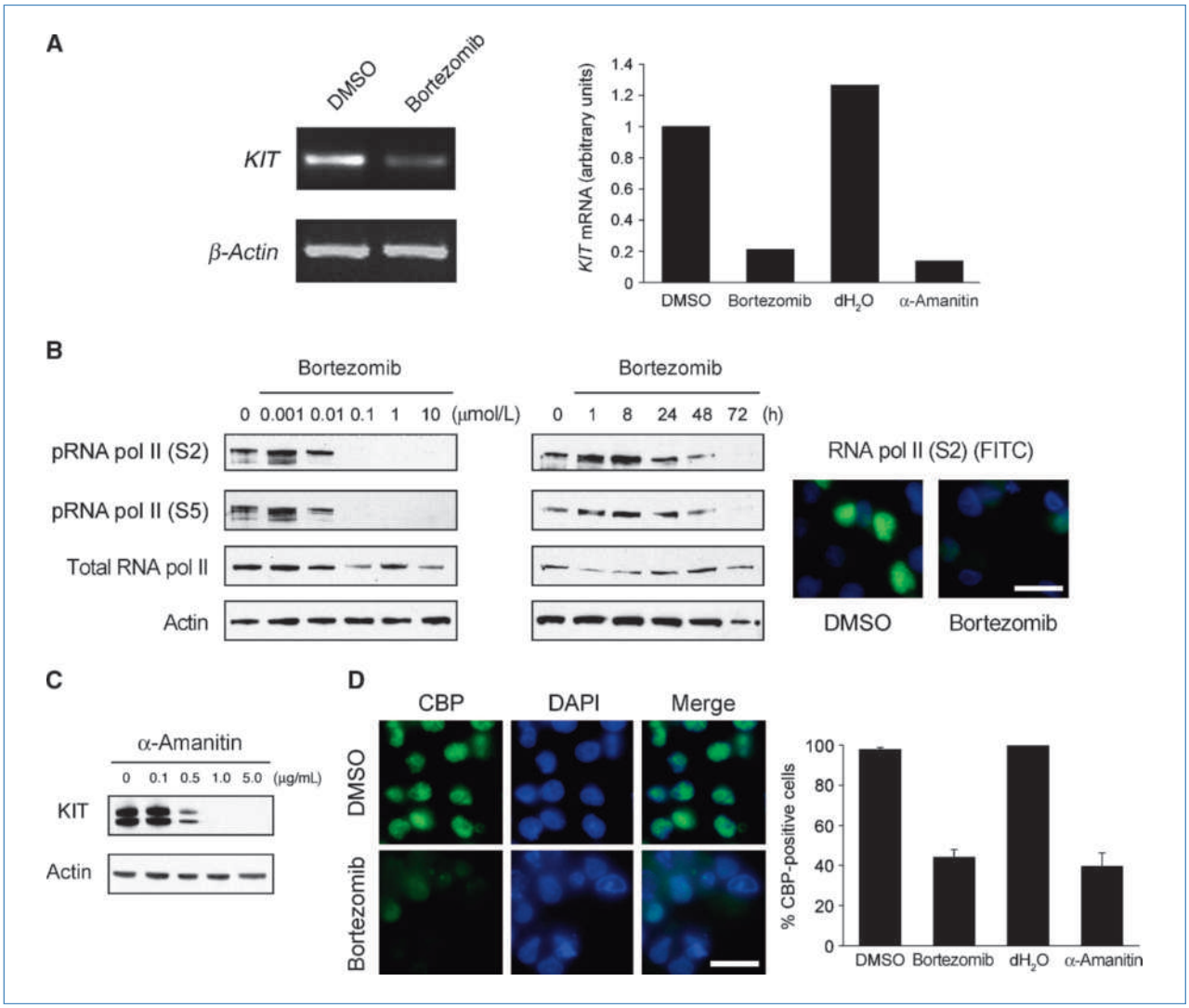

Figure 3. Bortezomib induces transcriptional inhibition of KIT. *A, left,* RT-PCR amplification of *KIT* mRNA after treating GIST882 cells with DMSO or 0.01 μmol/L bortezomib for 48 h. RT-PCR amplification of *β-actin* mRNA is shown to demonstrate loading. *Right,* qRT-PCR of *KIT* mRNA after treatment of GIST882 with DMSO/bortezomib (0.01 μmol/L) or dH_2O/α-amanitin (1 μg/mL) for 48 h. Values are normalized against *β-actin* mRNA. *B,* immunoblot analysis of GIST882 cells treated with bortezomib at the concentrations indicated for 72 h (*left*) or with 0.01 μmol/L bortezomib for the indicated times (*middle*) and probed for phospho-RNA polymerase II (S2), phospho-RNA polymerase II (S5), and total RNA polymerase II. Immunoblot for actin is shown to demonstrate loading. *Right,* immunofluorescence microscopic analysis of GIST882 cells treated with DMSO or 0.01 μmol/L bortezomib for 48 h and stained for phospho-RNA polymerase II (S2). Nuclei were stained with DAPI. *Bar,* 20 μm. *C,* immunoblot analysis of GIST882 cells treated with α-amanitin at the concentrations indicated for 72 h and probed for KIT. Immunoblot for actin is shown to demonstrate loading. *D, left,* immunofluorescence microscopic analysis of GIST882 cells treated with DMSO or 0.01 μmol/L bortezomib for 48 h and stained for CBP. Nuclei were stained with DAPI. *Bar,* 20 μm. *Right,* quantification of the percentage of GIST882 cells showing nuclear staining for CBP treated with either DMSO/bortezomib (0.01 μmol/L) or dH_2O/α-amanitin (1 μg/mL) for 48 h. *Columns,* mean of at least 100 cells from three independent experiments; *bars,* SEM.

Collectively, these findings underscore that bortezomib has unique effects on *KIT* mRNA levels, global transcriptional activity, and KIT protein levels when compared with imatinib or 17-AAG, and that modulation of the NF-κB pathway does not play a major role in bortezomib-induced apoptosis in GIST cells.

Bortezomib induces apoptosis and downregulates KIT in imatinib-resistant GIST cells. We next determined the efficacy of bortezomib in imatinib-resistant GIST cells. GIST48 and GIST 430 are cell lines derived from imatinib-resistant human GISTs (21). Treatment of these cells with bortezomib at concentrations ranging from 0.001 to 0.25 μmol/L led to a significant reduction of cellular proliferation with IC_{50} values of 0.003 and 0.002 μmol/L for GIST48 and GIST430, respectively (Fig. 4*A* and *B, top left*). By contrast, the IC_{50} was not reached when treating GIST48 or GIST430 with imatinib at concentrations ranging from 0.001 to 10 μmol/L (Fig. 4*A* and *B, top left*). A dramatic 5- to 12-fold increase in apoptosis was seen in GIST48 and GIST430 cells after 48 hours of treatment at concentrations of 0.005 to 0.02 μmol/L (Fig. 4*A* and *B, bottom left*). These data were confirmed by flow cytometry and Annexin V

Published OnlineFirst December 22, 2009; DOI: 10.1158/0008-5472.CAN-09-1449

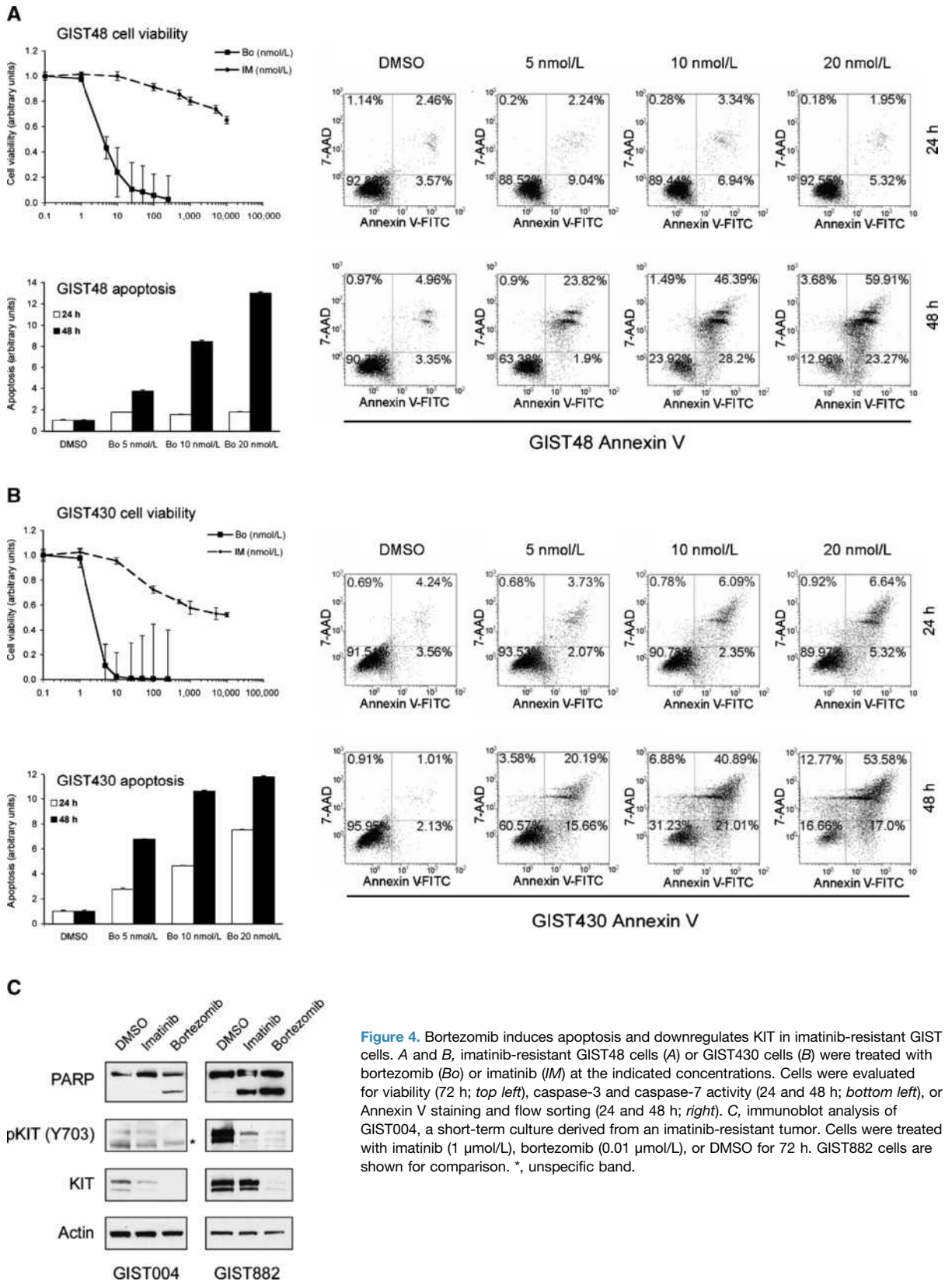

Figure 4. Bortezomib induces apoptosis and downregulates KIT in imatinib-resistant GIST cells. *A* and *B,* imatinib-resistant GIST48 cells (*A*) or GIST430 cells (*B*) were treated with bortezomib (*Bo*) or imatinib (*IM*) at the indicated concentrations. Cells were evaluated for viability (72 h; *top left*), caspase-3 and caspase-7 activity (24 and 48 h; *bottom left*), or Annexin V staining and flow sorting (24 and 48 h; *right*). *C,* immunoblot analysis of GIST004, a short-term culture derived from an imatinib-resistant tumor. Cells were treated with imatinib (1 μmol/L), bortezomib (0.01 μmol/L), or DMSO for 72 h. GIST882 cells are shown for comparison. *, unspecific band.

Published OnlineFirst December 22, 2009; DOI: 10.1158/0008-5472.CAN-09-1449

staining at the same concentrations and time points (Fig. 4*A* and *B, right*).

These preclinical validations of bortezomib as a novel therapeutic option in imatinib-resistant GIST were extended through evaluations in primary cultures established from an imatinib-resistant GIST. Mutational analysis of this tumor revealed a primary KIT exon 11 deletion (del550-558) and a secondary imatinib-resistant mutation in exon 14 (T670I). Short-term cultures were treated with 0.01 μmol/L bortezomib or 1 μmol/L imatinib for 72 hours. As shown by immunoblotting, bortezomib induced apoptosis in these cells as indicated by PARP cleavage, whereas imatinib had only a minor effect (Fig. 4*C*). Moreover, levels of phospho-H2AX and total H2AX increased after bortezomib treatment (data not shown). In concordance with our previous results, KIT and phospho-KIT (Y703) were downregulated after bortezomib treatment, whereas levels of KIT protein as well as KIT phosphorylation were largely unchanged when treated with imatinib (Fig. 4*C*).

Discussion

Although GISTs can be successfully treated with imatinib mesylate, new therapeutic options are needed because complete responses are rare and more than 80% of the patients develop resistance to the drug over time (4–6). Based on our previous finding that histone H2AX, which is causatively involved in the induction of apoptosis after imatinib, is regulated by the ubiquitin-proteasome machinery (14), we tested the possibility of using the FDA-approved proteasome inhibitor bortezomib for treating GIST. We found that bortezomib had a potent proapoptotic effect on GIST cells at the same concentrations used in multiple myeloma models, a disease for which bortezomib has clinical benefit (15, 16). Notably, the bortezomib-induced GIST apoptosis was preceded not only by upregulation of histone H2AX but also by downregulation of *KIT* oncogene mRNA levels.

Our current study supports the hypothesis that upregulation of histone H2AX by inhibition of the proteasome can induce apoptosis. However, downregulation of H2AX by siRNA only led to a moderate increase in surviving cells after bortezomib treatment (data not shown), suggesting that additional mechanisms are involved in the induction of apoptosis. Our finding that bortezomib treatment of GIST cells resulted in significant downregulation of KIT protein, accompanied by loss of KIT tyrosine phosphorylation, lends important support to this notion. It is known that loss of the KIT protein has a strong apoptotic effect in GIST cells as seen after knocking down KIT with siRNA or treatment with HSP90 inhibitors (14, 21). It is therefore likely that downregulation of KIT contributes substantially to the effect of bortezomib on GIST cells. Interestingly, downregulation of BCR-ABL in chronic myelogenous leukemia (CML) cells has been described after treatment with various proteasome inhibitors *in vitro* (25). Although the underlying mechanism was not shown, transcriptional inhibition was suggested as a potential explanation (25).

It is known that GISTs are especially prone to transcriptional inhibition (26). We have shown previously that treatment with the RNA polymerase II inhibitor α-amanitin led to an apoptotic response in GIST882, whereas nontransformed fibroblasts were not affected (14). We show here that bortezomib causes a transcriptional downregulation of KIT (Fig. 3*A*). We show that bortezomib treatment is associated with an inhibition of the global transcriptional machinery, including downregulation of RNA polymerase II phosphorylation as well as loss of the transcriptional coactivator CBP from chromatin throughout the nucleus. These findings indicate that bortezomib leads to a general transcriptional shutdown rather than to a specific loss of RNA polymerase II from the KIT promoter. Interestingly, it has been shown in BCR-ABL–positive CML cells that combination treatment of bortezomib with flavoperidol leads to transcriptional inhibition and loss of phosphorylation of the COOH-terminal domain of RNA polymerase II (27). However, the effect of either agent given alone was less pronounced (27). The mechanisms by which bortezomib downregulates *KIT* oncogene transcription are incompletely understood. It is known that the 26S proteasome is associated with transcriptionally active genes and physically interacts with RNA polymerase II (28). In fact, several studies have shown that ubiquitin-proteasome machinery is involved in regulation of transcriptional activation (29, 30), with initial binding and subsequent proteasomal degradation of transcriptional activators being necessary to initiate transcription and transcriptional elongation (31–34).

The dichotomous effect that bortezomib has on H2AX and KIT expression levels can most likely be explained by differences in the mechanism of protein degradation between H2AX and KIT. H2AX is processed by the ubiquitin-proteasome system, and its levels increase after treatment with a proteasome inhibitor. However, the phosphorylation-dependent degradation of KIT is mediated by the lysosome (35). This process is unlikely to be inhibited by compounds that target the ubiquitin-proteasome machinery. Hence, bortezomib treatment does not affect ongoing KIT degradation, which, together with reduced transcription (Fig. 3), results in a significant loss of KIT protein expression.

Inactivation of NF-κB through retention in the cytoplasm is thought to be a key mechanism of bortezomib-induced apoptosis in multiple myeloma (16, 19). We provide evidence that inhibition of the NF-κB signaling pathway does not seem to play a major role in bortezomib-mediated GIST cell death (Supplementary Fig. S3).

It is likely that transcriptional inhibition of KIT expression is not the only mechanism leading to apoptosis in GIST cells after bortezomib treatment. We are currently testing whether bortezomib is involved in the regulation of chaperone proteins, such as HSP90 and HSP70, as well as chromatin modifiers, such as histone deacetylases, which could also result in the downregulation of KIT protein. Interestingly, bortezomib has been shown to modulate the abundance of DNMT1, a DNA methyl transferase, in acute myeloid leukemia cells, leading to changes in DNA methylation and gene expression (36). Although increased DNA methylation would not explain the transcriptional downregulation of *KIT*, a change in methylation patterns could lead to the reexpression of other cell cycle inhibitory or proapoptotic genes that were epigenetically silenced in GIST cells, thus providing additional antiproliferative or cytotoxic stimuli.

Published OnlineFirst December 22, 2009; DOI: 10.1158/0008-5472.CAN-09-1449

Because most imatinib-resistant GISTs develop secondary mutations within the *KIT* or *PDGFRA* kinase domains, novel therapeutic approaches that do not directly target these kinases are particularly important. The example of HSP90 inhibitors, which likewise lead to loss of KIT oncoprotein expression in GIST, supports this notion (21). In that respect, our results that bortezomib is effective against GIST cells harboring various resistance mutations, including the so-called gatekeeper mutation, seem especially promising.

Further support for this notion comes from preliminary experiments, in which we treated heterozygous Kit^{K641E} transgenic mice (37) with bortezomib. After 2 or 4 weeks of treatment, some resected tumors showed loss of Kit expression, downregulation of cyclin A, and upregulation of cleaved caspase-3 by immunoblotting of whole-cell lysates (data not shown). These promising results indicate that bortezomib indeed has an effect *in vivo*. However, a larger cohort of animals needs to be treated for a longer period of time to confirm these preliminary results.

In summary, we have shown that bortezomib induces apoptosis in imatinib-sensitive as well as imatinib-resistant GIST cells. We identified a dual mode of action for bortezomib, including stabilization of histone H2AX as well as transcriptional downregulation of KIT. Our results provide a compelling rationale for clinical trials to test the efficacy of bortezomib in GIST patients.

Disclosure of Potential Conflicts of Interest

No potential conflicts of interest were disclosed.

Acknowledgments

We thank Christopher L. Corless (Oregon Health and Science University, Portland, OR) for providing the mutational analysis of GIST004 and Saumendra Sarkar (University of Pittsburgh Cancer Institute, Pittsburgh, PA) for helpful discussions and sharing important reagents. Imatinib mesylate was generously provided by Novartis Pharma, Basel, Switzerland.

Grant Support

American Cancer Society grant RSG-08-092-01-CCG (A. Duensing), the GIST Cancer Research Fund (A. Duensing and J.A. Fletcher), The Life Raft Group (A. Duensing, S. Bauer, B.P. Rubin, and J.A. Fletcher), Deutsche Krebshilfe Max Eder Nachwuchsgruppenprogramm D/06/107335 (S. Bauer), Stiftung Kampf dem Krebs (S. Bauer), the Virginia and Daniel K. Ludwig Trust for Cancer Research (J.A. Fletcher), and NIH grant 1P50CA127003-02 (J.A. Fletcher). A. Duensing is supported by the University of Pittsburgh Cancer Institute and in part by a grant from the Pennsylvania Department of Health. The Department specifically disclaims responsibility for any analyses, interpretations, or conclusions.

The costs of publication of this article were defrayed in part by the payment of page charges. This article must therefore be hereby marked *advertisement* in accordance with 18 U.S.C. Section 1734 solely to indicate this fact.

Received 4/20/09; revised 9/18/09; accepted 10/14/09; published OnlineFirst 12/22/09.

References

1. Hirota S, Isozaki K, Moriyama Y, et al. Gain-of-function mutations of c-kit in human gastrointestinal stromal tumors. Science 1998;279:577–80.
2. Rubin BP, Singer S, Tsao C, et al. KIT activation is a ubiquitous feature of gastrointestinal stromal tumors. Cancer Res 2001;61:8118–21.
3. Heinrich MC, Corless CL, Duensing A, et al. PDGFRA activating mutations in gastrointestinal stromal tumors. Science 2003;299:708–10.
4. Demetri GD, von Mehren M, Blanke CD, et al. Efficacy and safety of imatinib mesylate in advanced gastrointestinal stromal tumors. N Engl J Med 2002;347:472–80.
5. Verweij J, Casali PG, Zalcberg J, et al. Progression-free survival in gastrointestinal stromal tumours with high-dose imatinib: randomised trial. Lancet 2004;364:1127–34.
6. Blanke CD, Demetri GD, von Mehren M, et al. Long-term results from a randomized phase II trial of standard- versus higher-dose imatinib mesylate for patients with unresectable or metastatic gastrointestinal stromal tumors expressing KIT. J Clin Oncol 2008;26:620–5.
7. Demetri GD, van Oosterom AT, Garrett CR, et al. Efficacy and safety of sunitinib in patients with advanced gastrointestinal stromal tumour after failure of imatinib: a randomised controlled trial. Lancet 2006;368:1329–38.
8. Demetri GD, Benjamin RS, Blanke CD, et al. NCCN Task Force report: management of patients with gastrointestinal stromal tumor (GIST)—update of the NCCN clinical practice guidelines. J Natl Compr Canc Netw 2007;5 Suppl 2:S1–29; quiz S30.
9. Goodman VL, Rock EP, Dagher R, et al. Approval summary: sunitinib for the treatment of imatinib refractory or intolerant gastrointestinal stromal tumors and advanced renal cell carcinoma. Clin Cancer Res 2007;13:1367–73.
10. Antonescu CR, Besmer P, Guo T, et al. Acquired resistance to imatinib in gastrointestinal stromal tumor occurs through secondary gene mutation. Clin Cancer Res 2005;11:4182–90.
11. Debiec-Rychter M, Cools J, Dumez H, et al. Mechanisms of resistance to imatinib mesylate in gastrointestinal stromal tumors and activity of the PKC412 inhibitor against imatinib-resistant mutants. Gastroenterology 2005;128:270–9.
12. Wardelmann E, Thomas N, Merkelbach-Bruse S, et al. Acquired resistance to imatinib in gastrointestinal stromal tumours caused by multiple KIT mutations. Lancet Oncol 2005;6:249–51.
13. Liu Y, Perdreau SA, Chatterjee P, Wang L, Kuan SF, Duensing A. Imatinib mesylate induces quiescence in gastrointestinal stromal tumor cells through the CDH1-2-p27Kip1 signaling axis. Cancer Res 2008;68:9015–23.
14. Liu Y, Tseng M, Perdreau SA, et al. Histone H2AX is a mediator of gastrointestinal stromal tumor cell apoptosis following treatment with imatinib mesylate. Cancer Res 2007;67:2685–92.
15. Bross PF, Kane R, Farrell AT, et al. Approval summary for bortezomib for injection in the treatment of multiple myeloma. Clin Cancer Res 2004;10:3954–64.
16. Hideshima T, Richardson P, Chauhan D, et al. The proteasome inhibitor PS-341 inhibits growth, induces apoptosis, and overcomes drug resistance in human multiple myeloma cells. Cancer Res 2001;61:3071–6.
17. Adams J, Palombella VJ, Sausville EA, et al. Proteasome inhibitors: a novel class of potent and effective antitumor agents. Cancer Res 1999;59:2615–22.
18. Orlowski RZ, Kuhn DJ. Proteasome inhibitors in cancer therapy: lessons from the first decade. Clin Cancer Res 2008;14:1649–57.
19. Hideshima T, Chauhan D, Schlossman R, Richardson P, Anderson KC. The role of tumor necrosis factor α in the pathophysiology of

Published OnlineFirst December 22, 2009; DOI: 10.1158/0008-5472.CAN-09-1449

human multiple myeloma: therapeutic applications. Oncogene 2001; 20:4519–27.
20. Duensing A, Medeiros F, McConarty B, et al. Mechanisms of oncogenic KIT signal transduction in primary gastrointestinal stromal tumors (GISTs). Oncogene 2004;23:3999–4006.
21. Bauer S, Yu LK, Demetri GD, Fletcher JA. Heat shock protein 90 inhibition in imatinib-resistant gastrointestinal stromal tumor. Cancer Res 2006;66:9153–61.
22. Corless CL, McGreevey L, Haley A, Town A, Heinrich MC. KIT mutations are common in incidental gastrointestinal stromal tumors one centimeter or less in size. Am J Pathol 2002;160:1567–72.
23. Rubin BP, Duensing A. Mechanisms of resistance to small molecule kinase inhibition in the treatment of solid tumors. Lab Invest 2006;86: 981–6.
24. Liu Y, Parry JA, Chin A, Duensing S, Duensing A. Soluble histone H2AX is induced by DNA replication stress and sensitizes cells to undergo apoptosis. Mol Cancer 2008;7:61.
25. Dou QP, McGuire TF, Peng Y, An B. Proteasome inhibition leads to significant reduction of Bcr-Abl expression and subsequent induction of apoptosis in K562 human chronic myelogenous leukemia cells. J Pharmacol Exp Ther 1999;289:781–90.
26. Sambol EB, Ambrosini G, Geha RC, et al. Flavopiridol targets c-KIT transcription and induces apoptosis in gastrointestinal stromal tumor cells. Cancer Res 2006;66:5858–66.
27. Dai Y, Rahmani M, Pei XY, Dent P, Grant S. Bortezomib and flavopiridol interact synergistically to induce apoptosis in chronic myeloid leukemia cells resistant to imatinib mesylate through both Bcr/Abl-dependent and -independent mechanisms. Blood 2004; 104:509–18.
28. Gillette TG, Gonzalez F, Delahodde A, Johnston SA, Kodadek T. Physical and functional association of RNA polymerase II and the proteasome. Proc Natl Acad Sci U S A 2004;101:5904–9.
29. Muratani M, Tansey WP. How the ubiquitin-proteasome system controls transcription. Nat Rev Mol Cell Biol 2003;4:192–201.
30. Lipford JR, Deshaies RJ. Diverse roles for ubiquitin-dependent proteolysis in transcriptional activation. Nat Cell Biol 2003;5:845–50.
31. Lonard DM, Nawaz Z, Smith CL, O'Malley BW. The 26S proteasome is required for estrogen receptor-α and coactivator turnover and for efficient estrogen receptor-α transactivation. Mol Cell 2000; 5:939–48.
32. Reid G, Hubner MR, Metivier R, et al. Cyclic, proteasome-mediated turnover of unliganded and liganded ERα on responsive promoters is an integral feature of estrogen signaling. Mol Cell 2003;11:695–707.
33. von der Lehr N, Johansson S, Wu S, et al. The F-box protein Skp2 participates in c-Myc proteosomal degradation and acts as a cofactor for c-Myc-regulated transcription. Mol Cell 2003;11:1189–200.
34. Kim SY, Herbst A, Tworkowski KA, Salghetti SE, Tansey WP. Skp2 regulates Myc protein stability and activity. Mol Cell 2003; 11:1177–88.
35. Masson K, Heiss E, Band H, Ronnstrand L. Direct binding of Cbl to Tyr568 and Tyr936 of the stem cell factor receptor/c-Kit is required for ligand-induced ubiquitination, internalization and degradation. Biochem J 2006;399:59–67.
36. Liu S, Liu Z, Xie Z, et al. Bortezomib induces DNA hypomethylation and silenced gene transcription by interfering with Sp1/NF-κB-dependent DNA methyltransferase activity in acute myeloid leukemia. Blood 2008;111:2364–73.
37. Rubin BP, Antonescu CR, Scott-Browne JP, et al. A knock-in mouse model of gastrointestinal stromal tumor harboring kit K641E. Cancer Res 2005;65:6631–9.

Published OnlineFirst December 22, 2009; DOI: 10.1158/0008-5472.CAN-09-1449

Cancer Research
The Journal of Cancer Research (1916–1930) | The American Journal of Cancer (1931–1940)

AACR American Association for Cancer Research

Proapoptotic Activity of Bortezomib in Gastrointestinal Stromal Tumor Cells

Sebastian Bauer, Joshua A. Parry, Thomas Mühlenberg, et al.

Cancer Res 2010;70:150-159. Published OnlineFirst December 22, 2009.